With the use of computer-controlled titrators, a rapid amount of data can be taken and accurate values for stability, denaturant $m°$ values, and Hill coefficients can be obtained over a wide variety of conditions. Hence, CD provides a nice complement to site-resolved methods such as complementary oligonucleotide hybridization,[24] hydroxyl radical footprinting,[25] or chemical modification[26] methods as described in previous folding studies of large ribozymes.

Acknowledgments

We thank Prof. Tao Pan without whose collaboration these studies would not have been conducted. This work was supported by grants from the NIH (R01GM57880 to T.R.S. and Tao Pan) and from the Cancer Research Foundation (T.R.S.).

[24] P. P. Zarrinkar and J. R. Williamson, *Science* **265,** 918 (1994).
[25] B. Sclavi, S. Woodson, M. Sullivan, M. R. Chance, and M. Brenowitz, *J. Mol. Biol.* **266,** 144 (1997).
[26] A. R. Banerjee and D. H. Turner, *Biochemistry* **34,** 6504 (1995).

[25] Fluorescence Assays to Study Structure, Dynamics, and Function of RNA and RNA–Ligand Complexes

By NILS G. WALTER and JOHN M. BURKE

Introduction

After absorbing a photon, some molecules, called fluorophores, reradiate energy with a different wavelength than the exciting light; if emission occurs with a delay in the nanosecond time range, this process is called fluorescence (if emission is longer lived, it is referred to as phosphorescence). Fluorescence-based assays have been increasingly used during the past 35 years to study structure–function relationships in biological macromolecules. The emission of fluorophores is highly sensitive to their immediate and, in some cases, distant environment, making them excellent probes to measure local as well as global structures and their changes. A low detection level (typically in the nanomolar concentration range, and under certain conditions, using instrumentation for spatial resolution, even down to a single molecule) and the ability to continuously yield a reporter signal enable sensitive real-time monitoring of dynamic processes in solution. In many cases, such processes are at the heart of understanding the function of biopolymers.

0076-6879/00 $30.00

Proteins carry intrinsic fluorophores in the form of their tryptophan and tyrosine residues. Some, such as photoreceptors or the green fluorescent protein, even contain or bind more efficient chromophores. In addition, proteins often can be labeled site specifically with synthetic extrinsic fluorophores, using side chains that allow a specific coupling chemistry, such as the primary amino group of lysine or the thiol group of cysteine. These options have led to numerous applications of fluorescence in protein analysis, surveyed in many excellent reviews.[1-8] In particular, fluorescence assays have allowed the dissection and evaluation of structural transitions in the reaction pathway of protein enzymes.[9] This type of information has proven difficult to obtain by more traditional biophysical methods, such as nuclear magnetic resonance (NMR) spectroscopy and X-ray crystallography.

Intrinsic fluorescence from the protein component has been used to kinetically and thermodynamically characterize the formation of a number of protein–RNA complexes. Among them are complexes of aminoacyl-tRNA synthetases with their cognate tRNAs,[10-12] of a translational repressor from T4 phage with the repressed mRNA,[13] of both the nucleocapsid protein[14] and the reverse transcriptase[15] from human immunodeficiency virus (HIV) with their natural ligand tRNA(3Lys), or of the Rev protein from HIV with its RNA binding element.[16]

The discovery of ribozymes in the early 1980s has drawn our attention to the nature of RNA as a structurally and functionally dynamic biopolymer that often plays an active role in interactions with its environment. As a result, efforts have increased in recent years to directly monitor RNA structural dynamics and function in solution. The most direct way to obtain

[1] A. Coxon and T. H. Bestor, *Chem. Biol.* **2,** 119 (1995).
[2] D. M. Jameson and W. H. Sawyer, *Methods Enzymol.* **246,** 283 (1995).
[3] P. Selvin, *Methods Enzymol.* **246,** 300 (1995).
[4] A. R. Holzwarth, *Methods Enzymol.* **246,** 334 (1995).
[5] L. Brand, ed., *Methods Enzymol.* **278** (1997).
[6] D. P. Millar, *Curr. Opin. Struct. Biol.* **6,** 637 (1996).
[7] Y. C. Lee, *J. Biochem.* **121,** 818 (1997).
[8] J. H. Lakey and E. M. Raggett, *Curr. Opin. Struct. Biol.* **8,** 119 (1998).
[9] K. A. Johnson, *Curr. Opin. Biotechnol.* **9,** 87 (1998).
[10] M. Baltzinger and E. Holler, *Biochemistry* **21,** 2460 (1982).
[11] M. Fournier, C. Plantard, B. Labouesse, and J. Labouesse, *Biochim. Biophys. Acta* **916,** 350 (1987).
[12] S. X. Lin, Q. Wang, and Y. L. Wang, *Biochemistry* **27,** 6348 (1988).
[13] K. R. Webster and E.K. Spicer, *J. Biol. Chem.* **265,** 19007 (1990).
[14] Y. Mely, H. de Rocquigny, M. Sorinas-Jimeno, G. Keith, B. P. Roques, R. Marquet, and D. Gerard, *J. Biol. Chem.* **270,** 1650 (1995).
[15] S. H. Trall, J. Reinstein, B. M. Wörl, and R. S. Goody, *Biochemistry* **35,** 4609 (1996).
[16] W. C. Lam, J. M. Seifert, F. Amberger, C. Graf, M. Auer, and D. P. Millar, *Biochemistry* **37,** 1800 (1998).

this information is by using fluorophores incorporated into RNA molecules. The goal of the present review is to show examples of how such molecules can be employed to yield unique information on structure, dynamics, and function of RNA and its interactions with ligands, using widely available synthesis strategies and fluorometer instrumentation. To help the reader understand its potentials and demands we first review the basic terminology of fluorescence spectroscopy.

Fluorescence Spectroscopy and Its Potentials

Fluorescence is an interaction of light with matter.[17] Absorption of a photon by a fluorophore causes its transition from a ground to an excited electronic state. The excited state has a certain lifetime. While remaining in the excited state, the fluorophore internally converts part of its original excitation energy into molecular motion (heat). When the fluorophore reverses to its ground state, this energy loss results in the so-called Stokes shift of the emission relative to the absorption wavelength. In principle, a fluorophore can be cycled indefinitely between ground and excited states, producing a continuous fluorescence signal.

Every fluorophore has its unique absorbance and emission spectrum (wavelength distribution). Its emission spectrum is a mirror image of the absorbance, Stokes shifted to longer wavelengths. This shift makes fluorescence detection very sensitive, since emitted light can optically be separated from scattered excitation light. An absorbance spectrum is normally measured as excitation spectrum, with the excitation wavelength varied and the emission wavelength fixed. Conversely, an emission spectrum is obtained with the emission wavelength varied and the excitation wavelength fixed.

In the excited state, the fluorophore is sensitive to its environment. It can lose its excitation energy in a variety of ways, most of them radiationless, resulting in a quenched fluorescence. Quenching can occur through collisional quenching, excited state reactions, static quenching, and energy transfer. In fact, many potential fluorophores, such as the natural nucleobases, are quenched so strongly in solution that their fluorescence normally cannot be observed. Typical fluorophores to be employed for fluorescent assays have a quantum yield (the ratio of the number of photons emitted to the number absorbed) of at least 10%.

Diffusional encounters between a fluorophore and a quencher result in collisional or dynamic quenching. A common dynamic quencher is molecular oxygen, which quenches nearly all known fluorophores. In addition, it

[17] J. R. Lakowicz, "Principles of Fluorescence Spectroscopy." Plenum Press, New York, 1983.

can chemically react with excited fluorophore species, such as electronic triplet states, causing irreversible chemical decay, or photobleaching. Thus, it is frequently necessary to physically or chemically remove dissolved oxygen from a fluorophore containing solution, in particular when high sensitivity is desired.

When the fluorophore and its quencher form a nonfluorescent ground state complex, static quenching results. On absorption of a photon, this complex immediately returns to the ground state without emission of fluorescence.

A special case of quenching is fluorescence resonance energy transfer (FRET; sometimes simply called fluorescence energy transfer). Here, the energy of the excited state is transferred from the donor fluorophore to an acceptor. The transfer occurs without the appearance of a photon, and is the result of direct dipole–dipole interactions between the interacting molecules. The acceptor itself often is a fluorophore, so that its unique emission can be detected in addition to a quenched donor emission. The efficiency of FRET depends on the extent of overlap of the donor emission spectrum with the acceptor absorption spectrum, the relative orientation of the donor and acceptor transition dipoles, and the distance between the two fluorophores. This latter property enables accurate measurement of distances in the range of 10–100 Å by FRET, a distance range well suited to probing RNA molecules.

All of these molecular processes limit the average amount of time, or lifetime, a fluorophore remains in the excited state. Measurements of the lifetime can, therefore, reveal the frequency of collisional encounters with quenching agents, the rate of excited state reactions, and the efficiency of energy transfer. Typical fluorophore lifetimes are in the range of 10 nsec, necessitating the use of high-speed electronic devices and detectors. An advantage of the fast time regime of fluorescence is that it is faster by several orders of magnitude than molecular motions and conformational rearrangements; a fluorescence emission event therefore, like a snapshot, contains information on the pseudostatic molecular environment of the fluorescent probe at a given point in time. As a result, time-resolved fluorescence measurements can yield statistical information on ensembles of fluorophores and their distributions between different states.

In addition to the processes described, apparent quenching can occur due to the optical properties of the sample. For example, reabsorbed fluorescence or turbidity can result in decreased fluorescence intensities. These effects are trivial and contain very little molecular information. They have to be avoided to obtain useful information. An advantage of fluorescence lifetime measurements is their insensitivity to these apparent quenching effects.

On excitation with polarized light, the emission of a fluorophore is also polarized. This polarization or anisotropy is a result of the selection of the absorbing fluorophores according to their orientation relative to the polarization plane of the excitation light (photoselection). If the excited fluorophore were completely immobile over its lifetime, the resulting emission would be completely polarized as well. Since this is normally not the case, the remaining anisotropy reveals the average angular displacement of the fluorophore that occurs between absorption and subsequent emission of a photon. This angular displacement depends on the rate and extent of rotational diffusion during the lifetime of the excited state. Rotational diffusion properties of the excited state, in turn, depend on the viscosity of the solvent, the rotational freedom of the probe itself, and the size and shape of the molecule to which it is attached. The latter property has made anisotropy measurements an indispensable tool to monitor the formation or the structural changes of biological complexes.

Instrumentation

It is important to be aware that an observed signal may not originate from the fluorophore of interest. One may detect background fluorescence from other sample components, light leaks, Raleigh or Raman scattering, and/or ordinary stray light from particles in the sample. To ensure that indeed the fluorophore of interest produces the signal, it is necessary to check some specific features such as the emission and excitation spectra of the sample. To obtain these spectra appropriate equipment has to be used, typically a spectrofluorometer.[17] We will discuss the commercially available instrumentation in some detail to reveal its potentials and to help beginners getting involved in fluorescence-based projects.

Basic Spectrofluorometer

To avoid misinterpretation of the obtained data, some attention has to be paid to the experimental details of the utilized spectrofluorometer. The basic principle of a modern spectrofluorometer is simple (Fig. 1). Light from a source, often a continuous xenon (Xe) arc lamp with a broad wavelength spectrum, is optically focused and guided through lenses, mirrors, a monochromator (typically a diffraction grating with a variable slit to select a wavelength band of defined width), a shutter, and an optional polarizer into the sample. Sample fluorescence perpendicular to the emission beam (to minimize the excitation light contribution) is collected by a lens and guided through another shutter, an optional polarizer, and a monochromator arrangement into a photomultiplier tube (PMT; converts individual photons into an electrical current) as detector.

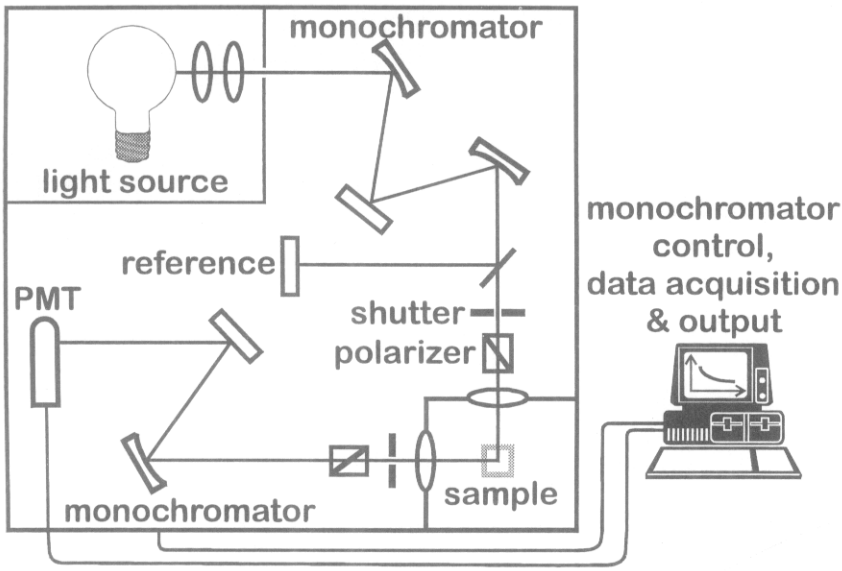

FIG. 1. The basic spectrofluorometer.

To increase the sensitivity of the signal, the wavelength and intensity of the excitation beam or the amplification of the emission signal can be varied. Because these parameters are adjusted from experiment to experiment, no absolute measurement of fluorescence intensity for a given sample is possible, and the assigned units will always be arbitrary. In addition, the observed excitation and emission spectra are dependent on the instrument on which they are recorded. Ideally, a spectrofluorometer should have an equal and constant photon output at all wavelengths, the monochromators should pass photons of all wavelengths and polarizations with equal efficiency, and the PMT should detect photons of all wavelengths with equal efficiency. However, an ideal spectrofluorometer does not exist, and variations of measured fluorescence spectra have to be expected from different instruments. To at least account for fluctuations in the excitation beam intensity, spectrofluorometers typically contain a beam splitter, passing a small fraction of the excitation light into a reference detector (Fig. 1).

Different types of commercial spectrofluorometers are available as either compact benchtop instruments or high-end modular devices that allow incorporation of alternative light sources such as pulsed lasers. In the course of projects it is often necessary to alter or extend the chosen approach, hence, versatile and easily upgradable equipment is desirable. We have performed our steady-state fluorescence experiments on an SLM/Aminco-Bowman series 2 (AB2, Spectronic Instruments, Rochester) spectrofluorometer benchtop instrument.

Optical Accessories

Depending on the desired application, accessories may be required for measuring spectroscopic qualities other than fluorescence intensity. For obtaining fluorescence lifetimes two techniques exist, the pulse method and the harmonic or phase-modulation method. In the pulse method the sample is excited by a very short light pulse, and the time-dependent decay of fluorescence intensity is recorded. Either flash lamps or pulsed lasers serve as light sources. The longer pulses (typically 2 ns) of flash lamps, on the one hand, make the correction (or deconvolution) of the observed fluorescence decay against the nonideal shape of the excitation pulse more challenging and limit the measurable lifetimes to >1 ns. Pulsed lasers with their <100-ps time pulses, on the other hand, are more demanding due to technical and cost considerations, but their versatility has led to an increasing popularity.

To obtain the entire time-resolved decay curve with sufficient accuracy, repetitive flash lamp or laser pulses have to be used. From the pulses, which have to be separated by at least five lifetimes to avoid overlap of their fluorescence responses, the complete decay curve can be constructed in two different ways. In the pulse sampling (or stroboscopic) method the gain of the PMT is briefly increased at a certain delay time after the excitation, yielding the sample fluorescence at that delay time. The fluorescence decay is obtained by sampling multiple excitation pulses, each for a different delay time. In the more widely used photon-counting method the detection system measures the time between the pulse and the arrival of the first photon. If the count rate is low enough to ensure the arrival of only a single photon per pulse, observing multiple pulses will, in total, reflect the time-resolved decay curve.

To measure lifetimes by the phase-modulation method the sample is excited with sinusoidally modulated light, and the phase shift and demodulation of the emission are used for calculating the lifetime. Light modulation is typically achieved by an ultrasonic modulator, and detection employs a cross-correlation mode. Because the lifetime is calculated indirectly from phase delay and demodulation factors, higher than first-order fluorescence decays will be averaged and both extremely short and long lifetimes can only be measured with considerable error, limiting the number of potential applications of the phase-modulation technique somewhat.

Fluorescence anisotropy measures the emission polarization from a fluorescent sample on excitation with fully polarized light, by calculating

$$\begin{aligned} A &= (I_{vv} - gI_{vh})/(I_{vv} + 2gI_{vh}) \\ g &= I_{hv}/I_{hh} \end{aligned} \tag{1}$$

where I_{vv}, I_{vh}, I_{hv}, and I_{hh} are the fluorescence intensities measured with excitation and emission polarizers subsequently in all four possible combi-

nations of vertical (v, 0°) or horizontal (h, 90°) alignment. To measure anisotropy, a relatively simple accessory is needed, namely, polarizers in both the excitation and emission pathways. Plastic film polarizers are often included in the basic setup of a spectrofluorometer, but they might not be appropriate for a given fluorophore because they absorb UV light. Other polarizers are made of UV-transparent prisms.

In principle, two techniques are in use for measuring fluorescence anisotropies, the L- and the T-format methods. In the L format, a single emission channel is used, and the emission polarizer is shifted between parallel and vertical positions with respect to the excitation polarization. In the T format, both positions are measured simultaneously using two separate detection systems, branching off in opposite perpendicular directions from the excitation beam. In both the L and T formats, the correction factor g [Eq. (1)] has to be calculated to compensate for the polarizing properties of the optical components, especially the monochromators.

The polarization properties of the optical components can also pose a problem for measuring accurate fluorescence intensities and lifetimes; if the anisotropy of the sample is changing, the observed fluorescence signal may change solely due to the dependence of the monochromators on the light polarization. Polarizers can be used to eliminate this polarization effect. Mathematically, it can be shown that the measured intensity becomes independent of the sample polarization if polarizers in the magic angle orientation are employed (with the excitation polarizer in the vertical position and the emission polarizer oriented 54.7° from the vertical).

Accessories for Kinetic Measurements

One particular advantage of fluorescence over alternative biophysical methods is its inherent capacity to produce continuous information on a reaction, revealing its kinetics. This "time resolution" must not be confused with the observation of a time-resolved fluorescence decay that describes the loss of excitation energy by fluorescence on a nanosecond timescale.

To be able to observe its kinetics, a reaction is typically initiated by mixing two reacting species. Manual mixing takes several seconds to ensure homogeneity, which might not be appropriate to observe a fast reaction. To overcome this problem, stopped-flow accessories have been developed for many spectrofluorometers. They contain at least two pressure-resistant syringes for the reagenets. Driven by a triggered hydraulic or pneumatic pressure system they inject their reagent solutions into a mixing chamber, from where the homogenized mixture is guided into the observation cell. The reagent flow stops abruptly when the exhaust syringe hits a physical barrier, and signal acquisition begins. The dead time before a fluorescence signal can be recorded is typically in the millisecond time range.

Traditionally, rapid stopped-flow equipment allows for continuous recording at a single defined emission wavelength only. Full excitation and emission spectra can only be taken after completion of the run. A more recent advancement of the stopped-flow technique is time-resolved spectrofluorometry.[18–21] Here, rapid emission wavelength scanning is accomplished by a dispersing element in the emission pathway, such as a monochromator with a spinning multiple-slit disk, a spinning grating, or an acousto-optic tunable filter, and the dispersed emission light is analyzed either with a PMT or a diode array. Depending on the setup, successive emission spectra can be recorded with high time resolution. These multiple-wavelength data potentially provide more information on the fluorescent intermediates of a reaction than a single-wavelength measurement does. Stopped-flow equipment can also be combined with the optical accessories described earlier to measure fluorescence lifetimes or anisotropies.

A different principle to analyze fast reaction kinetics is the relaxation method.[22] Here, a mixture of reagents in equilibrium with their reaction products is subjected to a sudden jump in a thermodynamic parameter influencing the equilibrium position, e.g., temperature or pressure. From the relaxation time back to the original equilibrium position the kinetics of the underlying reaction can be derived. If the reagents differ in their fluorescence properties from the products, relaxation can be followed by fluorescence measurements to obtain kinetic information.[23,24]

Instrumentation Yielding Spatial Resolution

Like most other biophysical methods, a typical measurement in a spectrofluorometer averages signals from all detectable molecules in an analyzed bulk volume. Fluorescence can, however, also yield detailed information about the spatial resolution of fluorescence from a sample, even down to the single-molecule level. Most prominent among the available techniques are the flow cytometer, where a laser excites a flowing fluid strem[25,26]; the fluorescence microscope to spatially resolve a distribution of fluorescing

[18] P. S. Brzovic and M. F. Dunn, *Methods Biochem. Anal.* **37,** 191 (1994).
[19] M. R. Eftink and M. C. R. Shastry, *Methods Enzymol.* **278,** 258 (1997).
[20] C. D. Tran and R. J. Furlan, *Anal. Chem.* **65,** 1675 (1993).
[21] T. Hartmann and A. S. Verkman, *Anal. Biochem.* **200,** 139 (1992).
[22] M. Eigen, *Q. Rev. Biophys.* **1,** 3 (1968).
[23] S. M. Coutts, D. Riesner, R. Romer, C. R. Rabl, and G. Maass, *Biophys. Chem.* **3,** 275 (1975).
[24] D. Labuda and D. Porschke, *Biochemistry* **19,** 3799 (1980).
[25] B. H. Villas, *Cell Vis.* **5,** 56 (1998).
[26] M. C. Roslaniec, C. S. Bell-Prince, H. A. Crissman, J. J. Fawcett, P. M. Goodwin, R. Habbersett, J. H. Jett, R. A. Keller, J. C. Martin, B. L. Marrone, J. P. Nolan, M. S. Park, B. L. Sailer, L. A. Sklar, J. A. Steinkamp, and L. S. Cram, *Hum. Cell* **10,** 3 (1997).

RNA molecules in live cells[27–31a]; and fluorescence correlation spectroscopy (FCS), where temporal autocorrelation of their fluorescence bursts yields information on the translational diffusion properties of individual fluorescent molecules traversing the sharp focus of a laser coupled to a confocal microscope.[32–35] Notably, spatial resolution of fluorescence signals is also a core technology in the rapidly developing fields of high-throughput screening for drug discovery[36,37] and chip-based hybridization assays for genome and expression pattern analysis.[38,39] Again, all of these techniques may be coupled with the optical accessories described earlier to yield further information, e.g., on fluorescence lifetimes or anisotropies.

Fluorescent RNA Derivatives

The most abundant bases in RNA are guanine, adenosine, uracil, and cytosine. These natural bases, however, do not fluoresce due to strong quenching in solution and cannot be used for fluorescence assays (except at biologically irrelevant, extremely low temperatures[40]). This lack in autofluorescence enables the background-free use of site-specifically incorporated fluorophores as probes for their local environment. RNA from natural sources sometimes carries suitable intrinsic fluorophores, in particular the

[27] X. F. Wang and B. Herman, "Fluorescence Imaging Spectroscopy and Microscopy." Wiley, New York, 1996.

[28] J. S. Ploem, *in* "Fluorescent and Luminescent Probes for Biological Activity," (W. T. Mason, ed.), p. 1. Academic Press, London, 1993.

[29] F. W. D. Rost, "Fluorescence Microscopy." Cambridge University Press, Cambridge, Massachusetts, 1992.

[30] F. W. D. Rost, "Quantitative Fluorescence Microscopy." Cambridge University Press, Massachusetts, 1991.

[31] D. Lansing Taylor, and E. D. Salmon, *Methods Cell. Biol.* **29,** 207 (1989).

[31a] P. Chartrand, E. Bertrand, R. H. Singer, and R. M. Long, *Methods Enzymol.* **318,** [33] (2000).

[32] N. L. Thompson, *in* "Topics in Fluorescence Spectroscopy," (J. R. Lakowitz, ed.), Vol. 1, p. 337. Plenum Press, New York, 1991.

[33] R. Rigler, *J. Biotechnol.* **41,** 177 (1995).

[34] P. Schwille, F. Oehlenschläger, and N. G. Walter, *Biochemistry* **35,** 10182.

[35] N. G. Walter, P. Schwille, and M. Eigen, *Proc. Natl. Acad. Sci. U.S.A.* **93,** 12805 (1996).

[36] L. Silverman, R. Campbell, and J. R. Broach, *Curr. Opin. Chem. Biol.* **2,** 397 (1998).

[37] J. G. Houston and M. Banks, *Curr. Opin. Biotechnol.* **8,** 734 (1997).

[38] M. Chee, R. Yang, E. Hubbell, A. Berno, X. C. Huang, D. Stern, J. Winkler, D. J. Lockhart, M. S. Morris, and S. P. Fodor, *Science* **274,** 610 (1996).

[39] L. Wodicka, H. Dong, M. Mittmann, M. H. Ho, and D. J. Lockhart, *Nat. Biotechnol.* **15,** 1359 (1997).

[40] V. Kleinwächter, J. Drobnik, and L. Augenstein, *Photochem. Photobiol.* **7,** 485 (1968).

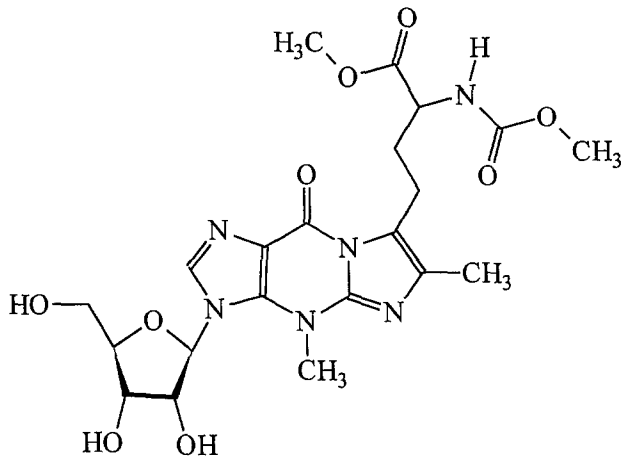

FIG. 2. Structure and fluorescence properties of the Wye base. Ex_{max}, excitation maximum; Em_{max}, emission maximum.

Wye (or Y) base (Fig. 2). This strongly modified guanine was extensively exploited in the 1980s to characterize structure, dynamics, and functional interactions of the anticodon loop of $tRNA^{Phe}$, using fluorescence intensity, anisotropy, and lifetime measurements of its Wye base.[41–46] However, the necessity to obtain the labeled RNA from natural sources and the fact that neither the nature of the fluorophore nor its attachment site can be manipulated have severely restricted applications of the Wye base.

With the invention of *in vitro* transcription using cloned RNA polymerases on defined DNA templates[47,48] and with the advancement of chemical

[41] N. Okabe and F. Cramer, *J. Biochem.* **89,** 1439 (1981).
[42] H. Paulsen, J. M. Robertson, and W. Wintermeyer, *J. Mol. Biol.* **167,** 411 (1983).
[43] W. Bujalowski, E. Graeser, L. W. McLaughlin, and D. Porschke, *Biochemistry* **25,** 6365 (1986).
[44] F. Claesens and R. Rigler, *Eur. Biophys. J.* **13,** 331 (1986).
[45] I. Gryczynski, H. Cherek, and J. R. Lakowicz, *Biophys. Chem.* **30,** 271 (1988).
[46] G. Striker, D. Labuda, and M. C. Vega-Martin, *J. Biomol. Struct. Dyn.* **7,** 235 (1989).
[47] J. F. Milligan and O. C. Uhlenbeck, *Methods Enzymol.* **180,** 51 (1989).
[48] S. van der Werf, J. Bradley, E. Wimmer, F. W. Studier, and J. J. Dunn, *Proc. Natl. Acad. Sci. U.S.A.* **83,** 2330 (1986).

solid-phase RNA synthesis,[49–52] two approaches became available in the 1980s to intently introduce fluorescent probes into a desired RNA. Subsequently, many covalent labeling strategies were developed to attach a variety of fluorophores.[53–56] We focus on fluorophores that are commercially available for site-specific attachment to chemically synthesized RNA. Although the length of chemically synthesized RNA at present is somewhat restricted due to limiting coupling efficiencies, the incorporation of a variety of additional nonnatural and modified nucleotides is possible, allowing for very flexible experimental strategies.

Labeling with Fluorophores during Chemical Synthesis

Chemical solid-phase synthesis of oligoribonucleotides has become a standard procedure in many molecular biology laboratories. Successful large-scale synthesis of RNA as long as 52 nucleotides has been described.[57] The chain is built from 3′ to 5′ end, starting from a solid-phase support, by repetitive cycles of condensation of 3′-activated and 5′-protected monomers with the growing chain. A few commercial suppliers exist, but our experience is that assembling the RNA oneself on an automated DNA/RNA synthesizer using commercially available β-cyanoethyl phosphoramidite activation chemistry is still the most reliable and versatile approach. Companies such as Glen Research (Sterling, VA), Applied Biosystems (Foster, CA), Pharmacia Biotech (Piscataway, NJ), Clontech (Palo Alto, CA), or ChemGenes (Waltham, MA) supply the required reaction chemistry together with phosphoramidites of unmodified and modified ribonucleotides and a variety of RNA modifiers including fluorescent probes. Automated DNA/RNA synthesizers are available from, e.g., Applied Biosystems, PerSeptive Biosystems (Framingham, MA), or Pharmacia Biotech. Our laboratory has had good experience with Glen Research chemistry on an Applied Biosystems 392 DNA/RNA synthesizer.

[49] K. K. Ogilvie, N. Usman, K. Nicoghosian, and R. J. Cedergren, *Proc. Natl. Acad. Sci. U.S.A.* **85,** 5764 (1988).
[50] F. Eckstein, ed., "Oligonucleotides and Analogues: A Practical Approach." Oxford University Press, United Kingdom, 1991.
[51] B. S. Sproat, *Curr. Opin. Biotechnol.* **4,** 20 (1993).
[52] R. H. Davis, *Curr. Opin. Biotechnol.* **6,** 213 (1995).
[53] A. Waggoner, *Methods Enzymol.* **246,** 362 (1995).
[54] C. Kessler, *J. Biotechnol.* **35,** 165 (1994).
[55] J. Temsamani and S. Agrawal, *Mol. Biotechnol.* **5,** 223 (1996).
[56] R. P. Haugland, "Handbook of Fluorescent Probes and Research Chemicals," (M. T. Z. Spence, ed.), 6th Ed. Molecular Probes, Eugene, Oregon, 1996.
[57] B. Sproat, F. Colonna, B. Mullah, D. Tsou, A. Andrus, A. Hampel, and R. Vinayak, *Nucleosides Nucleotides* **14,** 255 (1995).

Fluorophores that can be attached during synthesis need to be unreactive to coupling and deprotection chemistry. The currently most prominent fluorescent probes from Glen Research for attachment to RNA during synthesis are shown in Fig. 3, together with their basic fluorescence properties.

Fluorescein can be coupled to an RNA (1) 5′ terminally, in form of the chain-terminating 5′-fluorescein phosphoramidite; (2) internally, using either the fluorescein phosphoramidite with a removable 5′-DMT (dimethoxytrityl) protection group (creating an abasic site after coupling the next phosphoramidite) or fluorescein-deoxythymidine (dT) phosphoramidite (if a 2′-deoxythymidine can be tolerated); and (3) 3′ terminally, employing the fluorescein CPG solid-phase support to prime the synthesis (Fig. 3). In

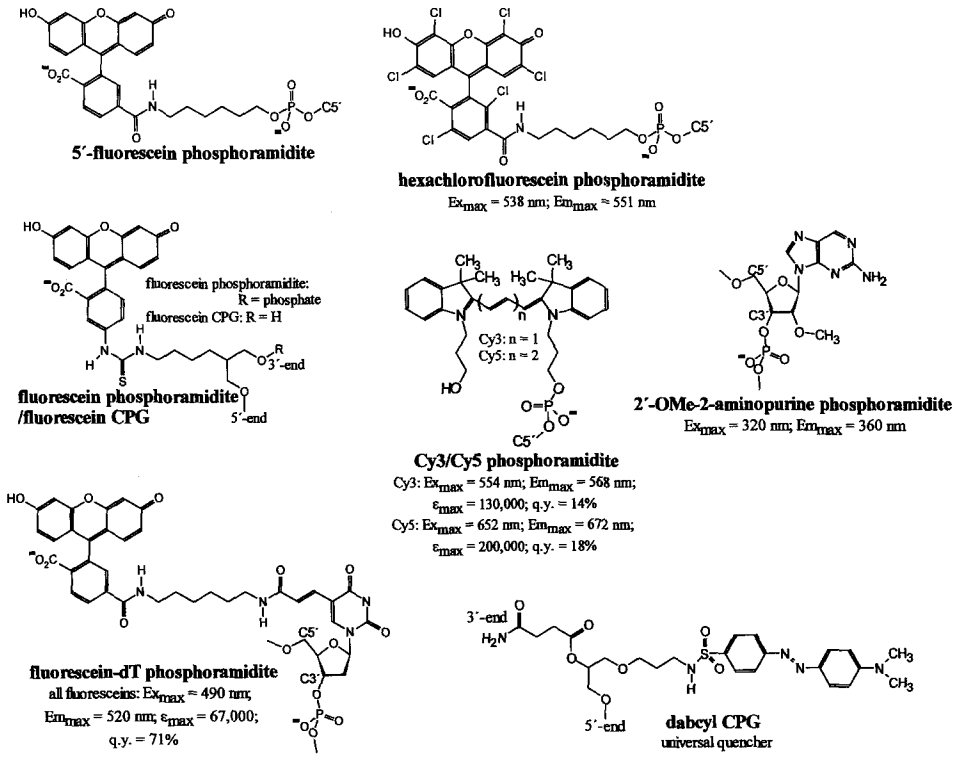

FIG. 3. Fluorophores for labeling during chemical RNA synthesis. The deprotected structures are shown, together with the names of their corresponding synthesis reagents. Typical fluorescence properties (may change after incorporation into RNA): Ex_{max}, excitation maximum; Em_{max}, emission maximum; ε_{max}, extinction coefficient at Ex_{max} [liter/(mol cm)]; q.y., quantum yield.

protein analysis, fluorescein has been the predominant green fluorophore for decades, due to its relatively high absorbance, near-optimal match to the 488-nm spectral line of the argon-ion laser, excellent fluorescence quantum yield, and good water solubility.[56] However, fluorescein is protonated below its pK_a 6.4, yielding a nonfluorescent acid form, and its relatively high photobleaching rate makes careful removal of dissolved oxygen from the reaction solution necessary to obtain a high detection sensitivity. A closely related dye, hexachlorofluorescein, is available as a phosphoramidite for 5′ end labeling of RNA (Fig. 3). Its six chlorine substituents shift its absorbance relative to fluorescein to longer wavelengths, enabling fluorescence resonance energy transfer (FRET) from the latter. We found hexachlorofluorescein to be sensitive against urea-induced hydrolysis so that oligoribonucleotides containing hexachlorofluorescein must not be purified on urea containing gels (see later discussion).

A different set of dyes to be utilized in RNA synthesis is the phosphoramidites of the cyanine derivatives Cy3 and Cy5 (Fig. 3). Even though they contain a removable MMT (4-monomethoxytrityl) protection group, Cy3 and Cy5 are not stable against repetitive synthesis cycles. They should be added at the 5′ terminus and the MMT group removed on the synthesizer. Due to its red-shifted absorbance spectrum, Cy3 is suitable as an acceptor for energy transfer from fluorescein.

2-Aminopurine (2AP; Fig. 3) is a fluorescent base analog of adenine. It base pairs with uracil in a structure isomorphous with an A-U Watson–Crick base pair. Currently, it is commercially available as the 2′-*O*-methyl-or 2′-deoxy-substituted phosphoramidite so that it can be internally incorporated only into RNA sites where modification of the 2′-hydroxyl group is tolerated. Several laboratories have worked out procedures to synthesize the ribose form of the phosphoramidite for studies in RNA.[58,59] 2-Aminopurine has the unique advantage that it directly reports on structural changes, especially in the base stacking pattern, around a single base, while most other fluorophores probe their environment in the minor or major groove of the nucleic acid double helix, depending on their attachment site.[60] In a DNA duplex, analysis of its fluorescence decay has shown that 2-aminopurine can be resolved into four differentially stacked species.[61]

One approach to analyze changes in nucleic acid structure is to observe

[58] M. Menger, T. Tuschl, F. Eckstein, and D. Porschke, *Biochemistry* **35,** 14710 (1996).

[59] B. B. Konforti, D. L. Abramovitz, C. M. Duarte, A. Karpeisky, L. Beigelman, and A. M. Pyle, *Mol. Cell* **1,** 433 (1998).

[60] D. P. Millar, *Curr. Opin. Struct. Biol.* **6,** 322 (1996).

[61] R. A. Hochstrasser, T. E. Carver, L. C. Sowers, and D. P. Millar, *Biochemistry* **33,** 11971 (1994).

an accompanying change in quenching of a site-specifically attached fluorophore. Altered fluorophore quenching may be brought about by a change in distance to a quencher and the probability of their collisional encounters. A site-specifically incorporated universal quencher that has been used for detection of DNA hybridization is dabcyl.[62] The 3′ terminus of a nucleic acid can be modified using the 3′-Dabcyl CPG solid-phase synthesis support from Glen Research (Fig. 3).

Postsynthetic Labeling with Fluorophores

Postsynthetic labeling with a site-specific fluorophore requires incorporation of a modification during synthesis that offers a unique postsynthetic coupling chemistry.[53] In use are primary alkylamino and alkylthiol modifications with different linker lengths. Site of modification can be the 5′ terminus, the 3′ terminus, and an internal position of the RNA, if the 5′ modifiers, 3′ modifiers, and a base-modified 2′-deoxythymidine are employed, respectively (Fig. 4A). The listed modifiers are stable against synthesis and deprotection chemistry. In the future, the development of additional labeling strategies can be expected, e.g., exploiting the 2′-hydroxyl groups and 3′,5′-phosphodiester linkages of RNA to attach fluorophores.

After synthesis and deprotection, primary amino groups can be specifically reacted with succinimidyl ester, isothiocyanate, or sulfonyl chloride groups on the fluorophore (Fig. 4B). Alkylthiol modifications on the RNA may be labeled using maleimide or iodoacetamide groups on the fluorophore, or in a disulfide exchange reaction (Fig. 4B). Many differnt reactive fluorophore derivatives, including appropriate labeling protocols for oligonucleotides, are available from Molecular Probes (Eugene, OR).[56] Typical labeling reactions are carried out over several hours under mild conditions at room temperature. A pH between 8.5 and 9.5 is required for coupling to alkylamino groups, since they need to be unprotonated; alkylthiols react in the range of pH 6.5–8.0. The absence of other (especially buffer) components with primary amino and thiol groups in the coupling reaction is essential to ensure specific attachment to the modified RNA. Incorporation of both an amino and a thiol group at different sites of the RNA enables two different fluorophores to be attached in separate labeling reactions, e.g., to observe FRET between them.

Two examples of reactive fluorophore derivatives to be attached postsynthetically are shown in Fig. 4C: the succinimidyl esters of pyrene and tetramethylrhodamine. Pyrene has an exceptionally long lifetime (up to

[62] S. Tyagi and F. R. Kramer, *Nature Biotechnol.* **14,** 303 (1996).

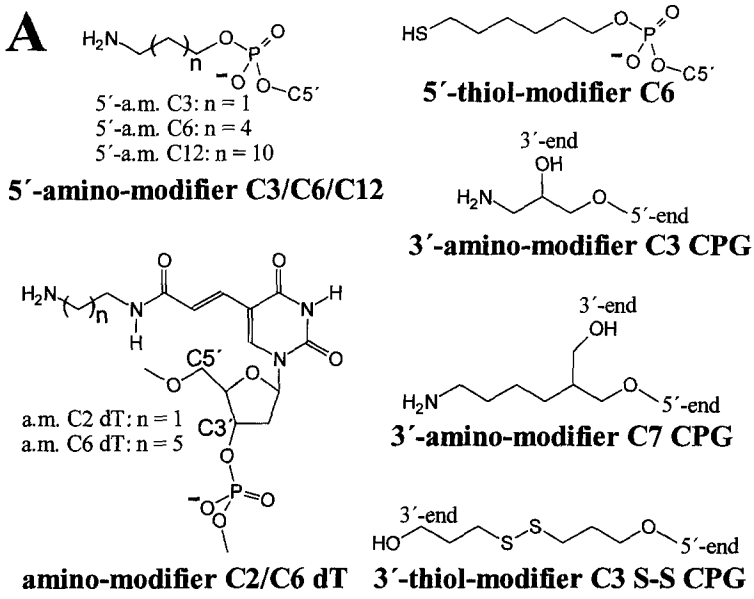

FIG. 4. Postsynthetic labeling of RNA with fluorophores. (A) Available alkylamino and alkylthiol modifiers. The deprotected structures are shown, together with the names of their corresponding synthesis reagents. (B) Labeling chemistry for alkylamino and alkylthiol modifications, respectively. (C) Exemplary fluorophores for postsynthetic labeling of synthetic RNA. Typical fluorescence properties (may change after coupling to RNA): Ex_{max}, excitation maximum; Em_{max}, emission maximum; ε_{max}, extinction coefficient at Ex_{max} [liter/(mol cm)]; q.y., quantum yield.

>100 ns) so that quenchers in its molecular environment have a particularly strong influence on the observed fluorescence. Tetramethylrhodamine is readily excited by the spectral lines of mercury-arc lamps and He–Ne lasers and is intrinsically more photostable than fluorescein.[56] It is a well-suited and widespread acceptor for FRET from fluorescein. Its conjugates with DNA have been shown to be able to populate multiple spectroscopic states, at least one of which is nonfluorescent.[63] A variety of closely related dyes with modified spectroscopic properties are available for oligonucleotide

[63] G. Vámosi, C. Gohlke, and R. M. Clegg, *Biophys. J.* **71,** 972 (1996).

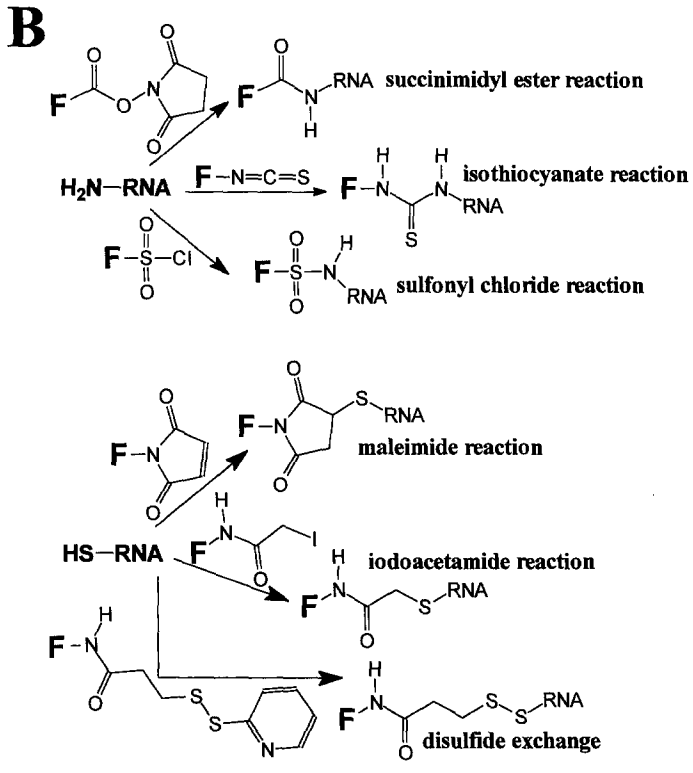

1-pyreneacetic(/butanoic) acid succinimidyl ester

Ex_{max} = 340 nm; Em_{max} = 385 nm;
ε_{max} = 29,000

5-carboxy-tetramethylrhodamine succinimidyl ester

Ex_{max} = 554 nm; Em_{max} = 573 nm;
ε_{max} = 85,000; q.y. = 28%

FIG. 4. (*continued*)

labeling from Molecular Probes (Eugene, OR), under names such as X-rhodamine, Texas Red, Rhodamine Red, and Rhodamine Green.[56]

Deprotection and Purification of Oligoribonucleotides

After synthesis, oligoribonucleotides need to be deprotected and purified. If they already contain fluorophores, these steps may require special precautions. We use a mild deprotection procedure that appears to be compatible with all fluorophores tested so far. It comprises (1) incubation for 4 hr at 65° in 1 ml of a 3:1 mixture of concentrated aqueous ammonia and ethanol (to remove the exocyclic amine protection groups), (2) drying in a lyophilizer, and (3) 20 hr of tumbling at room temperature with 800 μl triethylamine trihydrofluoride (to remove the 2′-OH-silyl protection groups).[64] Full-length RNA is recovered by precipitation with 1-butanol, drying, and purification on a denaturing (8 *M* urea) 20% polyacrylamide gel. For RNA containing hexachlorofluorescein, urea has to be omitted from the gel (see earlier discussion). Subsequent C_8 reversed-phase high-performance liquid chromatography (HPLC) in 100 m*M* triethylammonium acetate, with a linear elution gradient of 0–40% and 0–60% acetonitrile (50 min, 1 ml/min) for unlabaled and labeled strands, respectively, serves to remove material that is not fully deprotected. Under these conditions, fluorophore labeled RNA is considerably retarded relative to unlabeled RNA, due to its increased hydrophobicity. The elution gradients are chosen to elute the oligoribonucleotides between 14 and 20 min. If desired, fluorophores are coupled to alkylamino and alkylthiol groups at this stage. Subsequently, the labeled RNA is recovered by ethanol precipitation and several washes with 80% ethanol to remove residual reactive fluorophore, and is repurified by C_8-reversed-phase HPLC. One OD_{260} of the dried and resuspended HPLC peak fractions is assumed to correspond to a concentration of 37 μg/ml RNA. To obtain an accurate concentration for labeled RNA, the additional absorbances of the fluorophores at 260 nm should be taken into account with, e.g., $A_{260}/A_{492} = 0.3$ for fluorescein, $A_{260}/A_{535} = 0.3$ for hexachlorofluorescein,[65] and $A_{260}/A_{554} = 0.49$ for tetramethylrhodamine.[34] Alternatively, the RNA concentration can be calculated from the absorbance of the dye, e.g., using an extinction coefficient of 29,000 liter/(mol cm) for pyrene attached to pyrimidine bases.[66]

[64] B. Sproat, F. Colonna, B. Mullah, D. Tsou, A. Andrus, A Hampel, and R. Vinayak, *Nucleosides Nucleotides,* **14,** 255 (1995).

[65] K. P. Bjornson, M. Amaratunga, K. J. H. Moore, and T. M. Lohmann, *Biochemistry* **33,** 14306 (1994).

[66] R. Kierzek, Y. Li, D. H. Turner, and P. C. Bevilacqua, *J. Am. Chem. Soc.* **115,** 4985 (1993).

Examples of Fluorescence Assays for RNA

RNA Design

To initiate a project involving fluorescent RNA, the labeled strand has to be carefully designed. Site of attachment, linker length, and choice of fluorophore(s) have a strong influence on the observed fluorescence, enabling the rational design of probes for observing specific interactions in RNA. For example, it is well established that fluorescein and tetramethylrhodamine become specifically quenched by guanine bases in their local environment,[67,68] while pyrene is primarily quenched by pyrimidines.[69] Quenching is mediated by photo-induced electron transfer between the excited fluorophore and the base and largely depends on the frequency of their collisional encounters. Consequently, the length of the attachment linker and the hydrophobicity of the fluorophore as well as the structural flexibility of the base (that is altered on base pairing) determine the observed fluorescence signal.[70] These properties can be used to place a fluorophore at a site where it is likely to undergo a fluorescence change on a specific RNA structural change or ligand binding event of interest. Alternatively, an acceptor fluorophore or a quencher molecule can be site specifically attached to the RNA (or its ligand) to observe a similar effect. In this case, or if fluorescence anisotropy is measured to obtain information on the rotational diffusion properties of a labeled RNA, base-mediated quenching effects rather should be avoided to simplify data analysis.

General Considerations for Data Interpretation

Fluorescence measurements by necessity only yield relative values. Experiments to observe a specific RNA interaction, therefore, need to allow comparison of at least two signals, e.g., a change in fluorescence intensity, lifetime, or anisotropy upon addition or change of an essential cofactor (such as other RNA strands, ligands, or metal ions) has to be observed.

Once such a fluorescence signal change is observed, control experiments have to be performed to establish its origin, e.g., apparent quenching effects by stray or scatter light have to be ruled out. An elegant way to do so is to perform a titration with the added cofactor and record concentration dependent signal changes. The detection system parameters (including excitation and emission wavelengths) should be optimized for the highest possi-

[67] N. G. Walter and J. M. Burke, *RNA* **3,** 392 (1997).
[68] J. Widengren, J. Dapprich, and R. Rigler, *Chem. Phys.* **216,** 417 (1997).
[69] M. Manoharan, K. L. Tivel, M. Zhao, K. Nafisi, and T. L. Netzel, *J. Phys. Chem.* **99,** 17461 (1995).
[70] J. B. Randolph and A. S. Waggoner, *Nucleic Acids Res.* **25,** 2923 (1997).

ble signal quality. RNA concentrations need to be balanced between low reagent consumption and good signal quality. Ideally, several different fluorescence properties such as intensity, lifetime, and anisotropy should be measured to ensure correct interpretation of the data. Examples of successful applications of fluorescence spectroscopy in RNA biochemistry follow.

Monitoring Secondary Structure Formation by Fluorescence Quenching

Intriguing systems to study structure, dynamics, and function of RNA are ribozymes. Through their catalytic function, which involves dynamic folding transitions, they directly report on the presence of a biologically active structure. As a model system, we have studied the RNA folding pathways of the hairpin ribozyme, a reversible endonucleolytic motif from the negative strand of tobacco ringspot virus satellite and related viroid RNAs associated with plant viruses.[71–73] For biochemical studies *in vitro*, the satellite RNA has been truncated to about a 50-nucleotide ribozyme component that binds and cleaves a 14-nucleotide substrate *in trans*.[73] This construct, containing a two-way junction, has been used for targeted RNA inactivation within mammalian cells, and is the basis for experimental strategies in human gene therapy of genetic and viral diseases.[72]

To study reactions of the hairpin ribozyme, we developed a set of assays based on quenching of 3′-fluorescein-labeled substrates by a guanosine on the 5′ end of the substrate-binding strand of the ribozyme (Fig. 5A).[67] Addition of a ribozyme excess to the labeled substrate results in a decrease in steady-state fluorescence and an increase in anisotropy. We used the fluorescence quenching effect to monitor in real time the formation of the ribozyme–substrate complex, and to deduce the second-order substrate binding rate constant from a plot of the observed pseudo-first-order rate constants over a range of ribozyme concentrations.[67] Upon cleavage, the short 5′ and 3′ products rapidly dissociate so that the observed fluorescence increase reflects the cleavage rate constant. If a noncleavable substrate analog is used, its dissociation can be directly observed as a fluorescence increase after addition of a large excess of unlabeled noncleavable substrate analog as chase. From the ratio of the dissociation and binding rate constants, the equilibrium dissociation constant can be calculated to yield information on the thermodynamic stability of the ribozyme–substrate complex.[67,74]

[71] J. M. Burke, S. E. Butcher, and B. Sargueil, *Nucleic Acids Mol. Biol.* **10,** 129 (1996).
[72] D. J. Earnshaw and M. J. Gait, *Antisense Nucleic Drug Dev.* **7,** 403 (1997).
[73] N. G. Walter and J. M. Burke, *Curr. Opin. Chem. Biol.* **2,** 24 (1998).
[74] N. G. Walter, E. Albinson, and J. M. Burke, *Nucleic Acids Symp. Ser.* **36,** 175 (1997).

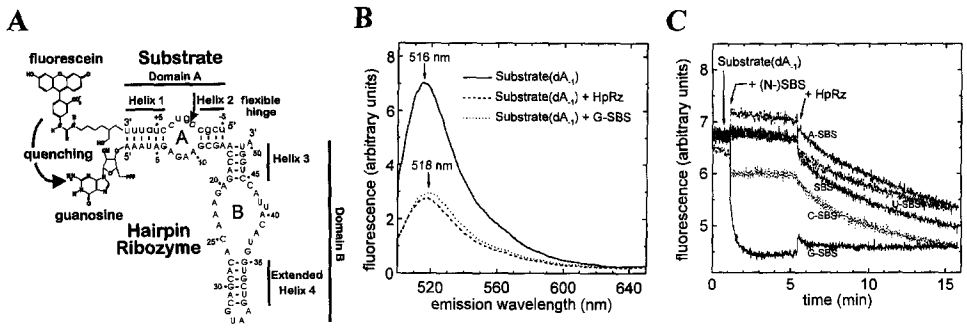

FIG. 5. Quenching assays to monitor secondary structure formation of the hairpin ribozyme–substrate complex. (A) The ribozyme–substrate complex (arrow, cleavage site in loop A). To observe fluorescence quenching on complex formation, fluorescein is coupled to the 3′ end of the substrate (small letters) so that it is located close to a dangling 5′-terminal G of the ribozyme (capital letters). (B) Steady-state fluorescence emission spectra of 10 n*M* fluorescein-labeled, noncleavable substrate analog (dA_{-1} modified) in standard reaction buffer (50 m*M* Tris-HCl, pH 7.5, 12 m*M* $MgCl_2$) at 25°, before (solid line) and after addition of a 10-fold excess of hairpin ribozyme (HpRz, dashed line) and substrate-binding strand with 5′ G (G-SBS, dotted line), respectively. Excitation was at 490 nm. After addition of HpRz or G-SBS, quenched steady-state fluorescence is observed, and the emission peak maximum is shifted slightly from 516 to 518 nm. (C) Base-specific quenching of fluorescein by guanosine. Fluorescence emission of 1 n*M* fluorescein-labeled, noncleavable substrate analog (dA_{-1} modified) under standard conditions was followed over time. After preincubation, a 10-fold excess was added of a substrate-binding strand either without (SBS) or with one of the four natural nucleosides at the 5′ end (G-SBS, U-SBS, C-SBS, A-SBS). Only G-SBS induces a quenching effect, resulting in an exponential signal decay on binding. Addition of all other substrate-binding strands leads to slightly altered, but stable fluorescence signals, due to changed scattering. After several minutes, addition of 10 n*M* hairpin ribozyme (HpRz) followed, resulting in a gradual displacement of the substrate-binding strands in the complexes by ribozyme. (From Walter and Burke.[67])

The about 55% decrease in steady-state fluorescence is also observed when an excess of isolated substrate-binding strand with a 5′-G is added to the 3′-fluorescein-labeled substrate (Fig. 5B). We were able to prove that the quenching is specifically mediated by the 5′-guanosine, because no other base on the substrate-binding strand exerts a similar effect (Fig. 5C). Figure 5C also demonstrates that the raw fluorescence signal may exhibit slight alterations that cannot be correlated with the structural change under investigation. Only careful control experiments (involving, e.g., addition or change of a cofactor) will prevent misinterpretation of the data.

Similar quenching assays have been utilized to monitor the formation and dissociation of a complex between a multiple-component ribozyme

derived from a group II intron and its 5′-fluorescein-labeled substrate.[75] Turner and co-workers used quenching of 5′-pyrene-labeled substrates to study the mechanism of substrate binding to the group I intron ribozyme from *Tetrahymena*.[66,76–78] From the biphasic binding kinetics at high substrate concentration, they were able to identify an open complex as a folding intermediate on the pathway to the fully tertiary structured closed complex. Finally, in the hammerhead ribozyme, quenching of site-specifically incorporated 2-aminopurine has been employed to observe ribozyme–substrate complex formation and subtle structural changes induced by local metal ion binding.[79]

Monitoring Tertiary Structure Formation by FRET

Fluorescence resonance energy transfer (FRET) has been used as a "molecular ruler" for biopolymers to estimate, under physiological (and other) conditions, distances in the range of 10–100 Å between a donor and a matching acceptor fluorophore.[3,5,60,80–84] The efficiency E of energy transfer is defined as the fraction of donor molecules de-excited through energy transfer to be acceptor, and can be calculated from the donor fluorescence intensities in the presence (I_{DA}) and absence (I_D) of the acceptor

$$E = (1 - I_{DA}/I_D) \tag{2}$$

Förster showed that transfer efficiency and fluorophore distance are linked by

$$E = 1/(1 + R^6/R_0^6) \tag{3}$$

where R is the donor-acceptor distance and R_0 is the Förster distance, at which 50% of the donor energy is transferred.[85]

Using this relationship, FRET has been employed to analyze the three-

[75] P. Z. Qin and A. M. Pyle, *Biochemistry* **36,** 4718 (1997).
[76] P. C. Bevilacqua, R. Kierzek, K. A. Johnson, and D. H. Turner, *Science* **258,** 1355 (1992).
[77] D. H. Turner, Y. Li, M. Fountain, L. Profenno, and P. C. Bevilacqua, *Nucleic Acids Mol. Biol.* **10,** 19 (1996).
[78] Y. Li and D. H. Turner, *Biochemistry* **36,** 11131 (1997).
[79] M. Menger, T. Tuschl, F. Eckstein, and D. Porschke, *Biochemistry* **35,** 14710 (1996).
[80] R. M. Clegg, *Methods Enzymol.* **211,** 353 (1992).
[81] P. Wu and L. Brand, *Anal. Biochem.* **218,** 1 (1994).
[82] R. M. Clegg, *Curr. Opin. Biotechnol.* **6,** 103 (1995).
[83] C. G. dos Remedios and P. D. Moens, *J. Struct. Biol.* **115,** 175 (1995).
[84] M. Yang and D. P. Millar, *Methods Enzymol.* **278,** 417 (1997).
[85] C. R. Cantor and P. R. Schimmel, "Biophysical Chemistry," Vol. 2, p. 448. Freeman, San Francisco, 1980.

dimensional structure of the hammerhead ribozyme, by calculating the FRET efficiency E from the extracted donor and acceptor contributions to the steady-state fluorescence spectra of doubly labeled ribozyme–substrate complexes.[86] The resulting model, however, although in general agreement with the global shape as determined by X-ray crystallography, was subsequently shown to predict an incorrect relative orientation of two of its three helical arms.[87] FRET has also been used to observe the bending of RNA helices containing bulge loops of varying length,[88] and to analyze global structure changes on metal ion titration in the hammerhead[89] and hairpin ribozymes[90,91] and in RNA four-way junctions.[92]

Several problems are associated with the use of FRET for determining absolute distances in nucleic acids: (1) Quenching of the fluorophores by RNA bases complicates data analysis. Because different structures have to be compared to obtain reliable dimensions, special care has to be taken to keep the sequence close to the fluorophores and their linker lengths identical between constructs. However, because subtle tertiary structure changes also may have an influence on the local environment of the dyes, identical fluorophore quenching between constructs is difficult to ensure. (2) For calculations of FRET distances one has to assume that the probes are able to undergo free, isotropic motion.[83] The high fluorescence anisotropy values for some fluorophore–nucleic acid conjugates indicate significant interactions between the dye and either bases or the negatively charged backbone of the nucleic acid.[63,86] Such interactions can be expected to interfere with fluorophore mobility and to bias distance measurements.[83] (3) There is usually some uncertainty in the position of the FRET dyes due to the flexibility of their linker arm. These problems need to be addressed when intra- or intermolecular distances in biological macromolecules are to be measured accurately.

On the other hand, a unique advantage of fluorescence measurements over other biophysical methods is their ability to produce a continuous signal to report on dynamic processes in solution. If relative signal changes over time are observed for a single construct, kinetic rates for conformational transitions can be inferred, avoiding problems associated with abso-

[86] T. Tuschl, C. Gohlke, T. M. Jovin, E. Westhof, and F. Eckstein, *Science* **266,** 785 (1994).
[87] S. T. Sigurdsson, T. Tuschl, and F. Eckstein, *RNA* **1,** 575 (1995).
[88] C. Gohlke, A. I. H. Murchie, D. M. J. Lilley, and R. M. Clegg, *Proc. Natl. Acad. Sci. U.S.A.* **91,** 11660 (1994).
[89] G. S. Bassi, A. I. H. Murchie, F. Walter, R. M. Clegg, and D. M. J. Lilley, *EMBO J.* **16,** 7481 (1997).
[90] A. I. H. Murchie, J. B. Thomson, F. Walter, and D. M. J. Lilley, *Mol. Cell* **1,** 873 (1998).
[91] F. Walter, A. I. H. Murchie, J. B. Thomson, and D.M.J. Lilley, *Biochemistry* **37,** 14195 (1998).
[92] F. Walter, A. I. H. Murchie, D. R. Duckett, and D. M. J. Lilley, *RNA* **4,** (1998).

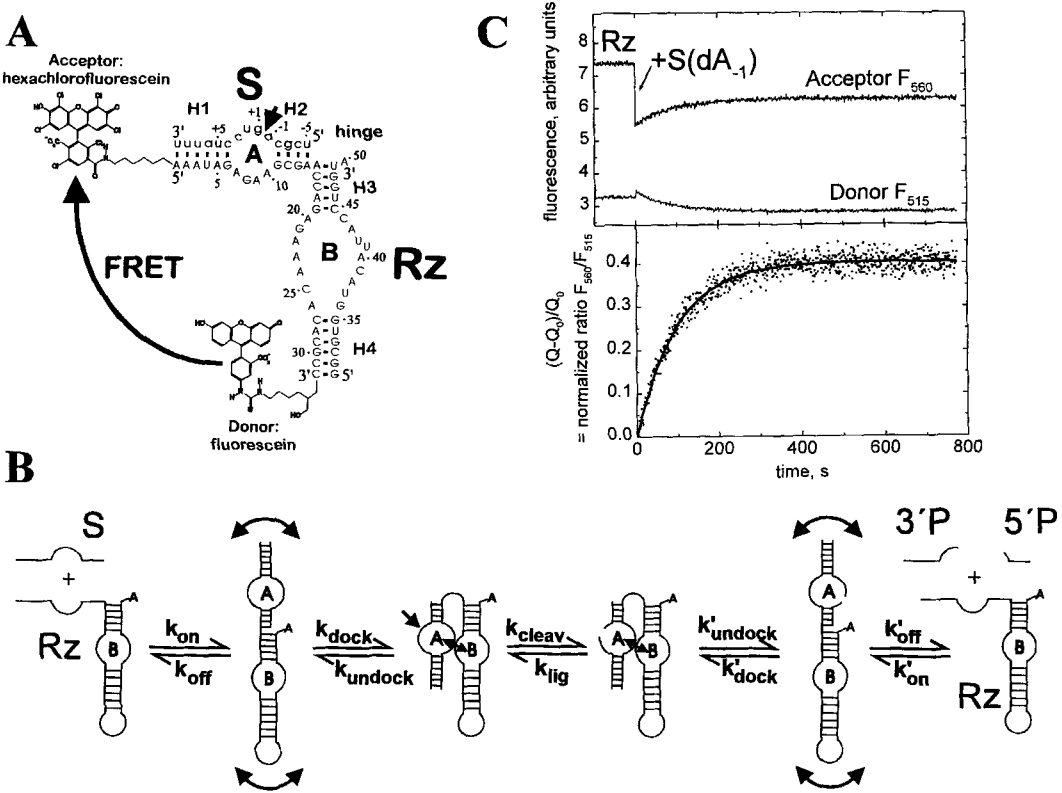
A
Acceptor:
hexachlorofluorescein
S
H1
H2
hinge
H3
H4
FRET
Rz
Donor:
fluorescein
C
Rz
+S(dA-1)
Acceptor F560
Donor F515
fluorescence, arbitrary units
(Q-Q0)/Q0 = normalized ratio F560/F515
time, s
B
S
Rz
kon
koff
kdock
kundock
kcleav
klig
k'undock
k'dock
k'off
k'on
3′P
5′P

lute distance measurements. We, therefore, developed a FRET-based assay to monitor in real time the reversible folding (docking) of the hairpin ribozyme–substrate complex from an open into a tertiary structured, closed conformation (Fig. 6).[93] In fact, we were able to measure accurately kinetic rate constants for this change in global structure under a variety of conditions, including modifications to the substrate and ribozyme, changes in metal ion composition, temperature, and pH. We found that docking precedes both cleavage and ligation reactions (Fig. 6B), but is rate limiting only for ligation. Strikingly, most modifications to the RNA or reaction conditions that inhibit cleavage do so by preventing docking, emphasizing the importance of RNA tertiary structure transitions for biological function.[93]

Of course, FRET can also be utilized to observe secondary structure formation in RNA, by placing a suitable donor–acceptor pair at sites that become close on association of complementary strands. Goodchild and coworkers have used this approach to measure the kinetics of formation and dissociation of hammerhead ribozyme–substrate complexes, and to answer

[93] N. G. Walter, K. J. Hampel, K. M. Brown, and J. M. Burke, *EMBO J.* **17,** 2378 (1998).

FIG. 6. Studying the kinetics of tertiary structure folding of the hairpin ribozyme–substrate complex by FRET. (A) The doubly labeled ribozyme–substrate complex. Fluorescein and hexachlorofluorescein are coupled as donor and acceptor pair to the 3′ and 5′ ends of the 5′ half of the two-strand ribozyme (Rz, capital letters) to enable distance-sensitive FRET (curved arrow). Short arrow, potential cleavage site in the substrate (S, small letters). (B) Minimal reaction mechanism for hairpin ribozyme catalysis as revealed by FRET. Substrate *in trans* is bound by the ribozyme into an open extended conformation, which subsequently folds into a docked bent structure, enabling loops A and B to interact. Site-specific cleavage follows (short arrow), the complex unfolds into an open complex, and the 5′ and 3′ cleavage products (5′P, 3′P) dissociate. All steps are fully reversible and can be characterized by individual rate constants. (C) Fluorescence signals over time as a result of tertiary structure folding of the ribozyme–substrate complex. The doubly labeled ribozyme, excited at 485 nm, displays a strong signal for the acceptor fluorophore at 560 nm and a weaker one for the donor at 515 nm. On manual addition of a saturating excess of noncleavable substrate analog (dA_{-1} modified), the acceptor fluorescence drops due to base-mediated quenching in the ribozyme–substrate complex. Subsequently, the acceptor signal increases, while the donor signal decreases at the same rate, indicating enhanced energy transfer efficiency between them. The normalized ratio Q of the acceptor:donor fluorescence as a measure for relative FRET efficiency was least-squares fitted with the equation $y = y_0 + A(1-e^{-t/\tau})$, yielding a first-order reaction rate constant of $1/\tau = 0.61$ min^{-1} with $A = 0.40$ and $\chi^2 = 0.00032$ (solid line). Conditions were 200 n*M* S(dA_{-1}) and 20 n*M* Rz (with a 10-fold excess of the unlabeled 3′ strand) in 50 m*M* Tris-HCl, pH 7.5, 12 m*M* $MgCl_2$, 25 m*M* dithiothreitol (DTT), at 25°. (From Walter *et al.*[93])

the question about how facilitator oligonucleotides might improve the turnover of substrate cleavage.[94]

Analyzing Conformational Isomers by Time-Resolved FRET

In principle, the strong dependence of FRET on the donor–acceptor distance [Eq. (3)] can be utilized to derive near-Ångstrom resolution of dimensions in a biopolymer. However, the intrinsic flexibility of nucleic acids and the fluorophore attachment linkers will give rise to distance distributions within the ensemble of analyzed molecules. Albaugh and Steiner[95] have demonstrated how these distance distributions can be derived experimentally from the associated multiexponential decay of the donor fluorescence. Millar and co-workers have applied this time-resolved FRET (tr-FRET) technique to the analysis of global structures of DNA three- and four-way junctions,[84,96] and were able to demonstrate that DNA four-way junctions typically can be resolved into equilibrium mixtures of two conformational isomers.[97]

We have studied the equilibrium distributions of hairpin ribozyme–substrate complexes between the active docked and inactive extended conformers by tr-FRET (Fig. 7). To avoid base-mediated quenching of the analyzed donor fluorescence (see earlier discussion), a guanosine-free sequence proximal to fluorescein in the complex was chosen (Fig. 7A). To derive distance information, two time-resolved fluorescence decays were collected, one for the sample with acceptor in place, one under identical conditions, but employing a donor-only RNA complex. Instrumentation comprised a mode-locked, 90-ps-pulse argon-ion laser for excitation at 514 nm, and perpendicular emission detection with polarizers in magic angle position, a 530-nm cutoff filter, and a single-photon counting photomultiplier.[96] The sample (150 μl) was incubated in the cuvette at measurement temperature for at least 15 min, prior to collecting >40,000 peak counts. The instrument response function to deconvolute the observed fluorescence decay was obtained using a dilute solution of nondairy coffee creamer to scatter the laser pulses. The decay of fluorescein emission in the doubly labeled complex was analyzed by a model of fluorophore distance distributions.[97]

[94] T. A. Perkins, D. E. Wolf, and J. Goodchild, *Biochemistry* **35,** 16370 (1996).
[95] S. Albaugh and R. F. Steiner, *J. Phys. Chem.* **93,** 8013 (1989).
[96] P. S. Eis and D. P. Millar, *Biochemistry* **32,** 13852 (1993).
[97] S. M. Miick, R. S. Fee, D. P. Millar, and W. J. Chazin, *Proc. Natl., Acad. Sci. U.S.A.* **94,** 9080 (1997).

$$I_{DA}(t) = \sum_k f_k \int P_k(R) \sum_i \alpha_i \exp\left[-\frac{t}{\tau_i}\left(1 + \left(\frac{R_0}{R}\right)^6\right)\right] dR \quad (4)$$

where the first sum refers to the number of distributions, either one or two, each with fractional population f_k and distance distribution $P_k(R)$. The distribution was modeled as a weighted Gaussian,

$$P(r) = 4\pi R^2 c \exp[-a(R - b)^2] \quad (5)$$

where a and b are parameters that describe the shape of the distribution and c is a normalization constant. Equation (4) was used to fit experimental data by nonlinear least squares regression, with a, b, and f_k for each distribution as adjustable parameters. Two distance distributions were used for analysis when a single distribution failed to give a good fit, as judged by the reduced χ^2 value and by inspection of residuals. In all such cases the inclusion of a second distribution resulted in a dramatic improvement of the fit. The intrinsic donor lifetimes τ_i and decay amplitudes α_i were determined for each set of experimental conditions by a sum-of-exponentials fit to the donor intensity decay in the donor-only complex. The Förster distance R_0 of 55 Å was calculated from the overlap of the donor emission and acceptor absorbance spectra, and by assuming free, isotropic motion of the dyes.[96] The latter assumption was supported by time-resolved fluorescence anisotropy decay experiments,[96] which revealed large-amplitude rotational motions of both fluorescein and tetramethylrhodamine, characterized by half cone angles of 28° and 42°, respectively.

Using this approach, we were able to distinguish ribozyme–substrate complexes, where domains A and B do not dock to a detectable (≥2%) extent (such as those with a substrate mutation $G_{+1}A$; Fig. 7B), from those that can perform this essential tertiary structure transition, as required for catalytic activity (Fig. 7C). The equilibrium distributions between docked and extended conformers in the latter complexes were used to describe the folding energy landscape of the hairpin ribozyme, and have helped to understand the role of the interdomain junction in stabilizing docking.[97a]

Observing Ligand Binding to RNA

Several approaches exist to analyze binding of ligands to RNA by fluorescence methods. Few have made use of fluorescent RNA, while many more employ fluorescent ligands. If the ligand is a protein, its intrinsic fluorescence often can be utilized to infer binding and dissociation kinetics and the equilibrium dissociation constant (as mentioned in the Introduc-

[97a] N. G. Walter, J. N. Burke, and D. P. Millar, *Nat. Struct. Biol.* **6**, 544 (1999).

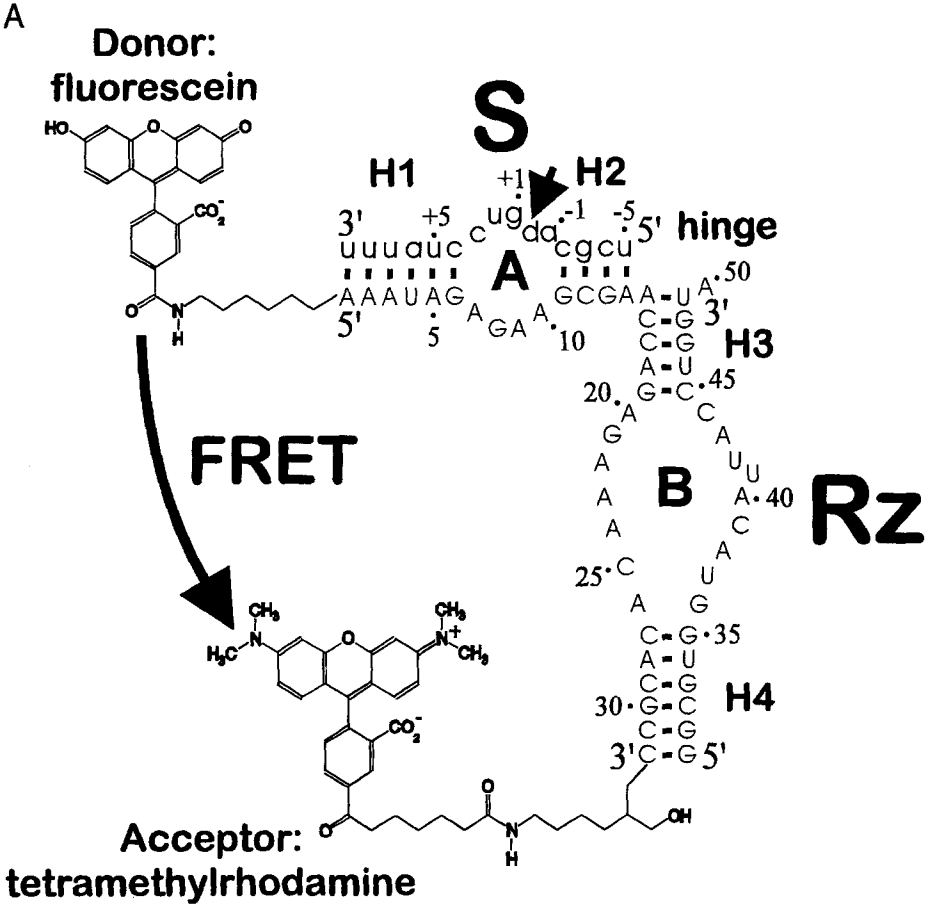

FIG. 7. Resolution of conformer distributions of the hairpin ribozyme–substrate complex using time-resolved fluorescence resonance energy transfer (tr-FRET). (A) The basic doubly labeled ribozyme–substrate complex. Fluorescein and tetramethylrhodamine are coupled as donor and acceptor pair to opposite ends of the ribozyme (Rz, capital letters) to enable distance-dependent FRET (curved arrow). Short arrow, potential cleavage site in the substrate (S, small letters). Cleavage is blocked by a dA_{-1} modification. (B) Revealing a single conformer by tr-FRET. A $G_{+1}A$ mutant substrate impairs docking of the ribozyme–substrate complex and results in a flexible extended conformer with fluorescein (F) and tetramethylrhodamine (T) at distant ends. The time-resolved donor (fluorescein) fluorescence decay of this complex under standard conditions (50 m*M* Tris-HCl, pH 7.5, 12 m*M* $MgCl_2$, at 17.8°) is measured and the donor–acceptor distance information extracted. A single continuous, three-dimensional Gaussian distance distribution (dashed line) fits the data very closely (giving a reduced χ^2 of 1.08). (C) Revealing an equilibrium between two conformers by tr-FRET. If the complex can fold from the initial extended structure into the docked conformer (in the presence of a G_{+1} base) the donor decay data (dots) can only be fitted with the sum of two Gaussian distance distributions ($\chi^2 = 1.28$), revealing the presence of both docked and extended conformers (deconvoluted contributions to the donor decay represented by solid and dashed lines, respectively). The relative abundance of these isomers is obtained directly from the analysis and is reflected in the relative heights of the corresponding distance distributions. tr-FRET thus defines the equilibrium constant K_{dock} and the energetic difference between docked and extended conformers in the RNA folding energy landscape, ΔG_{dock}.

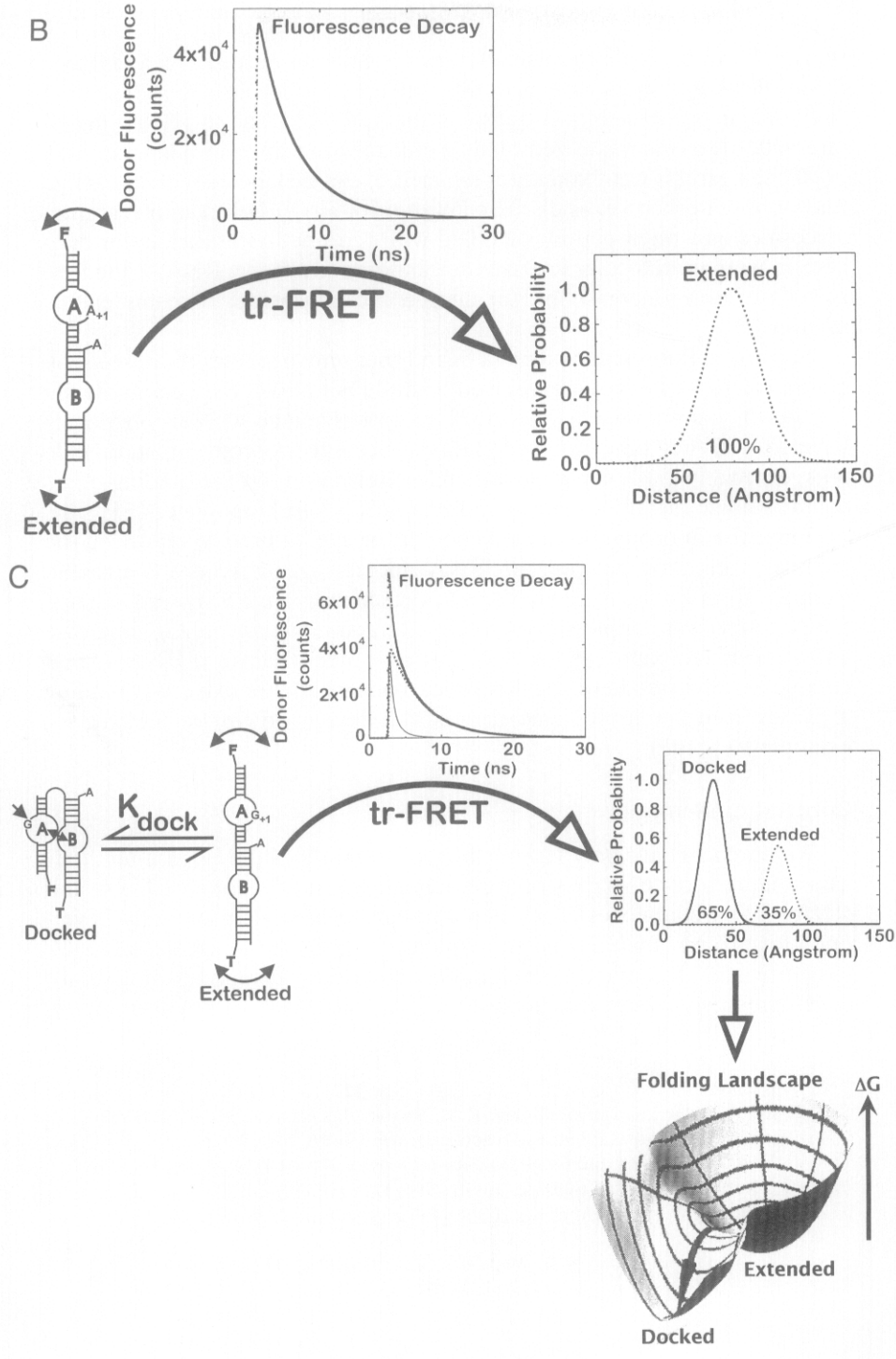

FIG. 7. (*continued*)

tion).[10–16] An example for a smaller intrinsically fluorescent ligand is riboflavin. RNA aptamers have been identified by *in vitro* selection that bind to riboflavin by virtue of a G-quartet structural motif, and the RNA–ligand interaction was characterized by fluorescence quenching in the complex.[98]

If the ligand is not fluorescent by itself, it can be labeled with a reactive fluorophore derivative, as discussed earlier for RNA. For example, aminoglycosides and small peptides labeled with tetramethylrhodamine or fluorescein were used to characterize their binding to specific RNA sequences, by measuring an increase in their fluorescence anisotropy on complex formation.[99,100]

Sensitized fluorescence from a ligand that only becomes fluorescent on binding to RNA has been employed to study binding of the lanthanide ion Tb^{3+} to the hammerhead ribozyme.[101] Horrocks and co-workers previously have shown that time-resolved fluorescence spectroscopy of lanthanide ions, especially Eu^{3+}, can yield valuable information on the binding mode of physiologic metal ions such as Mg^{2+} and Ca^{2+} to biopolymers.[102,103]

Finally, a fluorophore-labeled competitor can be used to report on the complex formation between an RNA and its ligand. Figure 8 gives an example from Preuss *et al.*, in which fluorescence from a 5′-pyrene-labeled DNA probe was employed to study interactions between Qβ replicase and various template RNAs.[104] As for all other studies on RNA–ligand complexes discussed here, the theoretical background for extracting binding affinities from the fluorescence data is well developed (for review, see for example Ref. 105).

Concluding Remarks

Researchers have only recently begun to embrace fluorescence methods as a unique tool to study structure, dynamics, and function of RNA and RNA–ligand complexes. They benefit from techniques previously developed for protein analysis and subsequently transferred to studies of DNA structure and dynamics. Combination of existing techniques and future developments in fluorescence-based technologies such as flow cytometry,

[98] C. T. Lauhon and J. W. Szostak, *J. Am. Chem. Soc.* **117,** 1246 (1995).
[99] Y. Wang, J. Killian, K. Hamasaki, and R. R. Rando, *Biochemistry* **35,** 12338 (1996).
[100] Y. Wang, K. Hamasaki, and R. R. Rando, *Biochemistry* **36,** 768 (1997).
[101] A. L. Feig, W. G. Scott, and O. C. Uhlenbeck, *Science* **279,** 81 (1998).
[102] W. D. Horrocks and D. R. Sudnick, *Science* **206,** 1194 (1979).
[103] D. Chaudhuri, W. D. Horrocks, J. C. Amburgey, and D. J. Weber *Biochemistry* **36,** 9674 (1997).
[104] R. Preuss, J. Dapprich, and N. G. Walter, *J. Mol. Biol.* **273,** 600 (1997).
[105] M. R. Eftink, *Methods Enzymol.* **278,** 221 (1997).

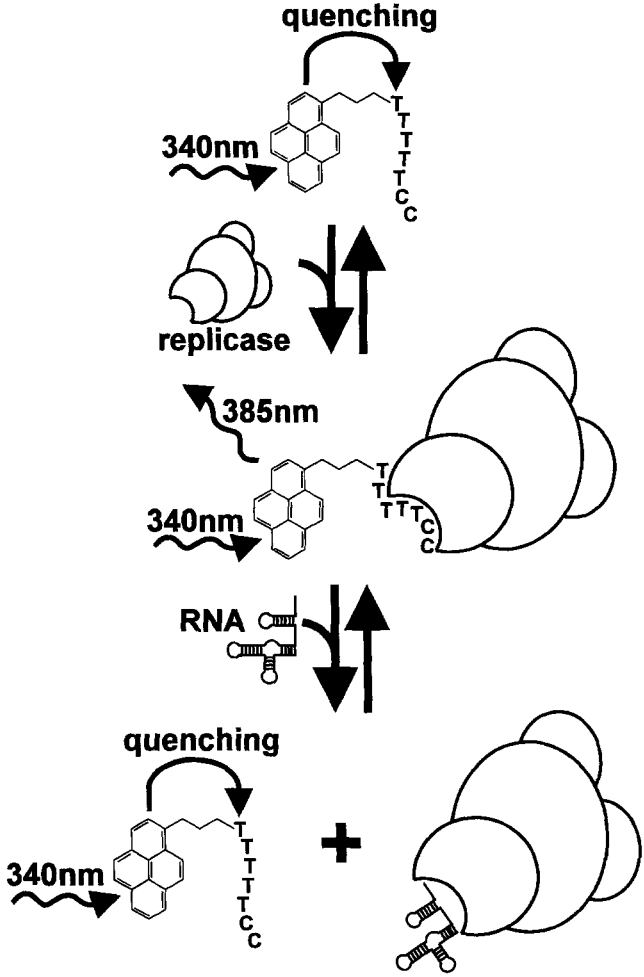

FIG. 8. Fluorometric reverse titration assay to observe binding of Qβ replicase to its template RNA. When free in solution, the 5′-pyrene-labeled DNA probe (excited at 340 nm) is strongly quenched through interactions between pyrene and its pyrimidine-rich sequence. On reversible binding of the heterotetrameric phage Qβ replicase to the probe, pyrene becomes dequenched and fluoresces with a peak around 385 nm. When template RNA is added, it partially displaces DNA probe in the complex (corresponding to the relative equilibrium binding constants of RNA and probe), resulting in a fluorescence decrease. (From Preuss *et al.*[104])

single-molecule fluorescence microscopy, high-throughput screening for drug discovery, and chip-based hybridization assays can be expected to have a strong impact on the extent to which the principles described in this review will be utilized.

Acknowledgments

This work was supported by grants from the U.S. National Institutes of Health to J.M.B., and a Feodor Lynen fellowship from the Alexander von Humboldt foundation and an Otto Hahn medal fellowship from the Max Planck Society for N.G.W.

[26] Transient Electric Birefringence for Determining Global Conformations of Nonhelix Elements and Protein-Induced Bends in RNA

By PAUL J. HAGERMAN

Introduction

Transient electric birefringence (TEB) is a sensitive method for characterizing both the conformations and the flexibilities of RNA molecules in solution. In its application to the study of RNA conformation, it is fundamentally a hydrodynamic method; RNA helices with central bends undergo more rapid rotational diffusion than do their linear counterparts because the bent molecules experience less frictional resistance. Because rotational diffusion is much more sensitive to changes in overall helix conformation than is translational diffusion, and because the relationship between the experimental diffusion constants and hydrodynamic theory is more straightforward, TEB has proven to be quite useful for quantifying both intrinsic and protein-induced bends in RNA (for a brief review, see Ref. 1). Another important distinction between rotational and translational diffusion pertains to the magnitude of the direct frictional contribution of a bound protein or element of RNA tertiary structure. For centrally placed elements, rotational diffusion is relatively insensitive to the frictional surface of the added protein or RNA structure since such elements lie close to the center of rotation. Thus, one does not generally require detailed knowledge of the shape of the bound protein or nonhelix element.

In a typical TEB experiment, an element of interest (e.g., branch, protein

[1] P. J. Hagerman, *Curr. Opin. Struct. Biol.* **6,** 643 (1996).

0076-6879/00 $30.00